Experiments in Fluids 27 (1999) 392–399

The study of self-sustained oscillating plane jet flow impinging upon a small cylinder

F.-B. Hsiao, Y.-W. Chou, J.-M. Huang

Abstract Experimental studies of a plane jet impinging upon a small circular cylinder are conducted by hot-wire measurements. The cylinder is located on the jet centerline within the potential-core region. The jet–cylinder interactions on the instability shear layer frequency, the cylinder wake shedding frequency, and the induced self-sustained oscillation phenomenon are carefully investigated. Test data indicate that the self-sustained flow oscillation is mainly generated by the resonant effect of the flow between the jet exit and the cylinder. Its resonant frequency is found to vary linearly and exhibits jump-stage pattern as a function of the distance between the jet exit and the cylinder. The feedback mechanism and the hydrodynamic instability theorem are proposed to predict correctly the frequency jump position, wave number and the convection speed of the self-sustained oscillating flow for different jet exit velocities.

List of symbols

a	sound speed
c	growth rate of the instability
d	cylinder diameter
$E(f)$	energy content of velocity fluctuations at specific frequency
f_0	fundamental frequency of the jet
f_r	resonant frequency
f_s	vortex shedding frequency of the cylinder wake
H	height of the plane jet at the exit
K	ratio of U_c and U_0
L	impinging length (distance from jet exit to cylinder front)
Re	Reynolds number ($=U_0H/\nu$)
$R_{\mathrm{I,II}}(\tau)$	cross-correlation function between the two sensors I and II
St	Strouhal number ($=fd/U_0$)
T_0	one period of a periodical signal
t	time scale
U	streamwise mean velocity
U_c	convection speed
U_0	mean velocity at the nozzle exit
u'	streamwise RMS velocity fluctuation
$u'(f)$	amplitude of streamwise velocity fluctuation at specific frequency
$v'(f)$	amplitude of transverse velocity fluctuation at specific frequency
X,Y	streamwise, transverse coordinate
X_{cy},Y_{cy}	streamwise, transverse coordinate of the cylinder
ν	kinetic viscosity
λ_0	initial instability wavelength of the jet ($=U_0/2f_0$)
λ_r	resonant instability wavelength ($=U_0/2f_r$)
ϕ_u	phase of the streamwise velocity fluctuation
$\Delta\phi_{\mathrm{I,II}}$	relative phase difference between the two sensors I and II
τ	time delay in the cross correlation function
α	wave number

Received: *15 July 1998*/*Accepted*: *9 December 1998*

F.-B. Hsiao, Y.-W. Chou
Institute of Aeronautics and Astronautics,
National Cheng Kung University
Tainan, Taiwan, R.O.C.

J.-M. Huang
Aeronautical Research Laboratory
Chung Shan Institute of Science and Technology
Taichung, Taiwan, R.O.C.

Correspondence to: F.-B. Hsiao

This work is supported by the National Science Council, R.O.C., under contract NSC 81-2212-E-006-018.

1 Introduction

A basic shear layer impingement flow field is formed when an obstacle is located in the downstream of a free shear flow. As the shear flow impinges upon a rigid surface, an induced periodic self-sustained oscillation can be observed by the interactions of the unstable shear layer and the downstream obstacle (Brackenridge 1960; Ho and Nosseir 1980; Rockwell and Kayayoglu 1986; Rockwell and Naudascher 1979). Powell (1961) pointed out that the acoustic disturbances near the vicinity of the impinging surface are the sources on radiating pressure fluctuations with specific tones, which lead to the transverse undulation of the impinging plane jet column. Such a self-sustained oscillating flow is found to perform jump and stage behaviors for the resonant frequency of the velocity and pressure fluctuations.

There are many combinations in the shear layer and solid body interacting flow studies. The shear layers may include jet, mixing layer and wake (planar or axisymmetric). The solid body may be sharp edge corner, flat (or curved) plate, wedge, orifice and cylinder. Most of the researches on jet–edge or the jet–plate interactions focused on the frequency jump and stage characteristics, and the dominant mechanism results in the self-sustained flow oscillation (Chanaud and Powell 1965;

Ho and Nosseir 1981; Rockwell and Kayayoglu 1986). A succession of events is observed to govern the occurrence of self-sustained flow oscillation: (i) impingement of organized vortical structures upon the solid body; (ii) upstream propagating disturbances; and (iii) subsequent amplification of the velocity fluctuations within the shear layers. In other words, the feedback effects from the interacting coherent structures at the impinging point can further excite the evolution of the shear layer upstream, such that the periodical shear oscillation can be obtained.

The conventional investigations on jet–cylinder impinging flow focused mainly on the mechanisms of vortex–edge interaction and the pressure fluctuation of the cylinder. The impinged cylinders usually have larger diameters as compared to the width (or spreading) of the jet column. The resonant frequency of the induced self-sustained flow oscillation observes to be coupled with the jet fundamental instability frequency. Recently, Chou et al. (1996) selected a "small" cylinder, which is placed downstream of the plane jet exit, to study the resulting jet–cylinder interaction behaviors. The major difference from the past studies is that the cylinder diameter is smaller than the width of the jet exit. In such a case, the downstream evolving coherent structures of the jet shear layer can no longer directly impinge upon the small cylinder as that for the conventional jet and "large" cylinder impingement. However, the self-sustained oscillating flow can still be observed under the jet and small cylinder impingement. Its resonant frequency here is not the fundamental frequency of the natural jet, f_0, but instead matches with the shedding frequency of the cylinder wake.

Up to now, the intrinsic characteristics of the wake shedding instability in the resonant self-sustained oscillating flow is still not clear for a small cylinder wake immersed in a jet column. In this paper, the flow structures and induction mechanisms of the self-sustained oscillating flow for a plane jet impinging upon a small circular cylinder are extensively studied. The Reynolds numbers effect in the flow filed is also examined in details.

2
Experimental facilities and data processing

The experiment is conducted in a plane jet with a height of 15 mm and an aspect ratio of 20 at the nozzle exit, as shown in Fig. 1. The jet facility is an open-circuit, blowing-down type wind tunnel. The air source of the jet is generated by a variable speed centrifugal blower. The turbulence intensity at the nozzle exit center is below 0.3% in the operating velocities of $U_0 = 5$–26 m/s. The corresponding Reynolds numbers based on the jet exit height, H, range between $5.02 \times 10^3 \sim 2.7 \times 10^4$.

The plane jet column can be divided into shear layer region and potential core region, as shown in Fig. 2(a). There are two cylinder diameters ($d = 3$ and 4 mm), which are relatively located in the downstream of the jet centerline, are employed in the present study of jet–cylinder impingement. The shedding frequencies measured in the cylinder wake under the jet velocity of $U_0 = 10$ m/s, are 700 Hz ($d = 3$ mm) and 500 Hz ($d = 4$ mm), respectively. The corresponding Reynolds numbers based on the cylinder diameter, d, are 2.07×10^4 ($d = 3$ mm) and 2.77×10^4 ($d = 4$ mm). Their calculated Strouhal numbers based on the shedding frequencies are 0.21 ($d = 3$ mm) and 0.2 ($d = 4$ mm), respectively. In most measurements here, the cylinder moves downstream along the centerline from the jet exit. The impinging length is then defined as the distance between the jet exit to the front surface of the cylinder. The arrangement of the impinged cylinder in the jet column is plotted in Fig. 2(b).

Two independent traversing mechanisms are used to control the positions of the cylinder and the measuring sensors. Their movements are computer-controlled with a spatial resolution of 0.02 mm. By using cross-type hot wire sensors, the streamwise and transverse velocity components in the flow field can be measured simultaneously. In some cases, a single-wire sensor is used as a reference signal source of velocity fluctuation. A 12-bit A/D converter associated with a PC computer is used for data acquisition and subsequent data processing. The mean velocity and fluctuation intensity are obtained by long-time average calculations. The FFT and the phase-average techniques are employed to perform the spectrum and vorticity analysis of the flow structures.

3
Results and discussion

3.1
The resonant frequency

For a natural jet, the initial most amplified instability wave is recognized to dominate the downstream evolution of the

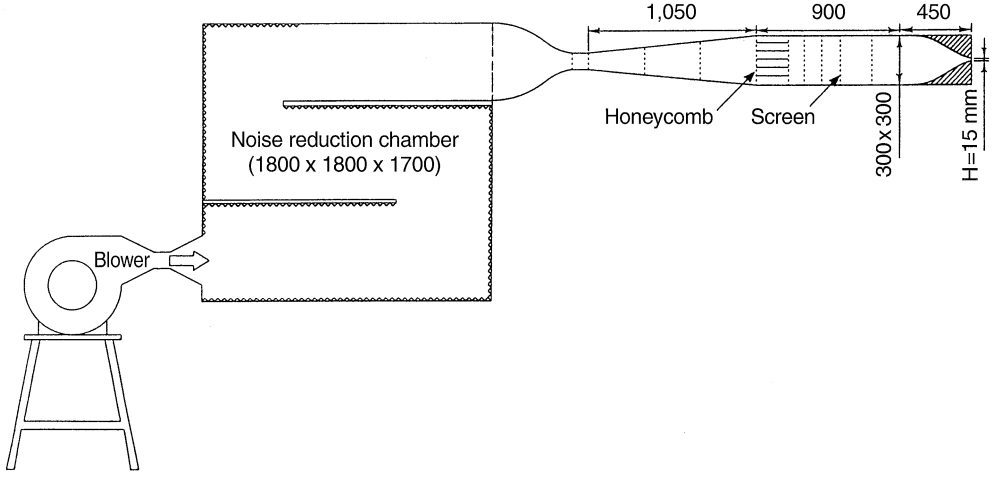

Fig. 1. Experimental layout of the plane jet

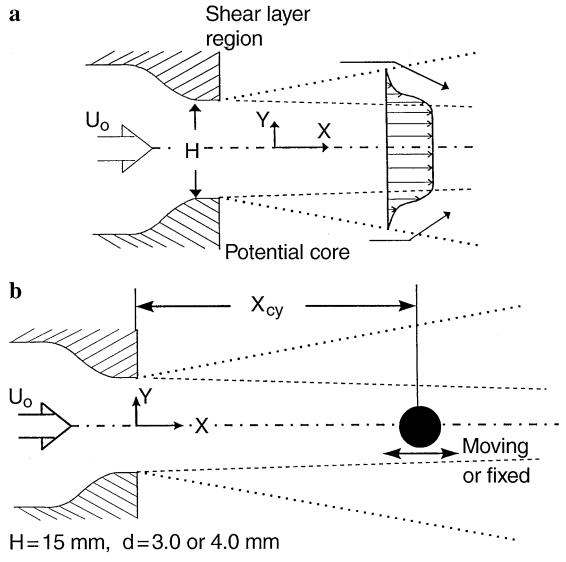

Fig. 2. Schematic representation of **a** the plane jet, and **b** the impinging jet flow field

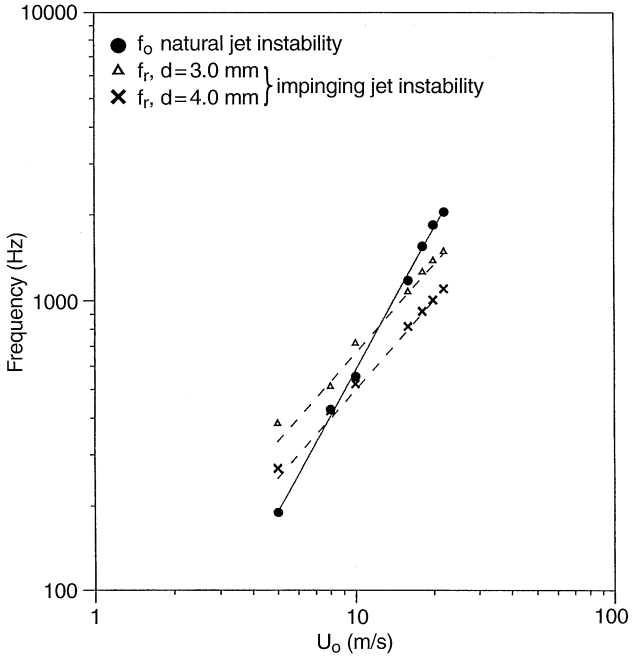

Fig. 3. Comparisons of fundamental frequency and resonant frequency with different jet exit velocities and $X_{cy}=0.5$ H. ●, △, ×: measured data, —: $f_0 \propto U_0^{3/2}$, … : $f_S \propto U_0$

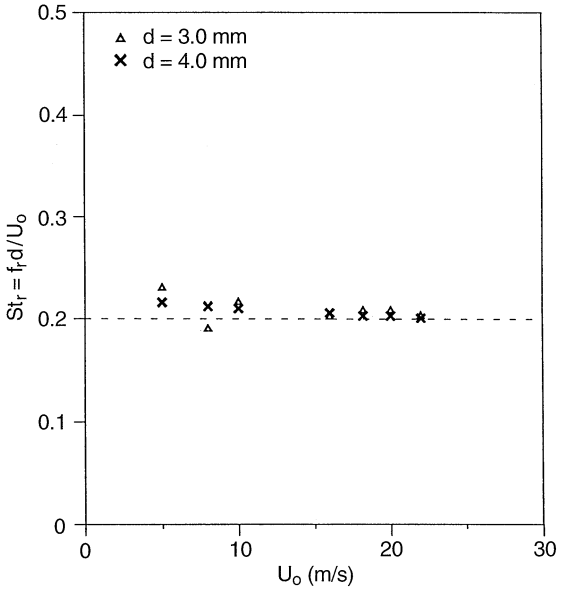

Fig. 4. Variations of resonant Strouhal number with different jet exit velocities and $X_{cy}=0.5$ H

coherent structures. Its fundamental frequency and the jet exit velocity is found to exhibit a relationship of $f_0 \propto U_0^{3/2}$, as shown in Fig. 3. As for the conventional cylinder wake flow, the organized shedding vortices could be clearly visualized in the range of $300 < Re < 10^5$(Roshko 1954). The vortex shedding frequency is now proportional to the freestream velocity, i.e., $f_s \propto U_0$. The non-dimensional Strouhal number, which is based on the vortex shedding frequency of the cylinder wake and the cylinder's diameter, keeps a constant value of about 0.2. The dashed lines in Fig. 4 illustrate the calculated results by $St_s = f_s d/U_0 = 0.212\ (1 - 12.7/Re)$ for both cylinder diameters of 3.0 and 4.0 mm. This clearly demonstrates the major differences of the dominant instability frequencies between the jet and the wake as a function of the operating velocities. When the circular cylinder is located at $X_{cy}=0.5H$ on the jet centerline, a cross-wire sensor is used to measure the frequency spectra at $2\lambda_0(\lambda_0 = U_0/2f_0) = 1.24\ H = 18.6$ mm. It is compared to that of the natural jet, as shown in Fig. 5. A pronounced peak at a characteristic frequency (i.e., the resonant frequency, f_r), at 700 Hz is observed for the impinging cylinder case, which is obviously distinct from the fundamental frequency of the natural jet. By varying the jet exit velocity, it can be found that the resonant frequency is fairly proportional to the jet exit velocity. That is

$$f_r \propto U_0$$

The results are further plotted in Fig. 3, and are compared with the instability frequency of the natural jet. It is noted that the resonant frequency is consistent with the calculated shedding frequency of the wake behind a circular cylinder, in which the corresponding Strouhal numbers, $St_r = f_r d/U_0$, are also well calculated around the constant value of 0.2, as shown in Fig. 4.

Earlier investigations by Lucas and Rockwell (1984) pointed out that the resonant frequency induced by the presence of an obstacle in a jet is identical to the fundamental frequency. In the present jet–small cylinder interacting flow study, as the cylinder is located within the potential core region, the evolution of the instability waves becomes dominated by the shedding frequency in the wake of a circular cylinder. The induced resonant frequency here is obviously not equal to the fundamental frequency of a plane jet. In fact, the disturbances generated by the shedding vortices of the cylinder act as an exciting source to govern the resonant frequency of the entire impinging jet flow field. On the other hand, as the cylinder is located further downstream, which is outside the jet potential

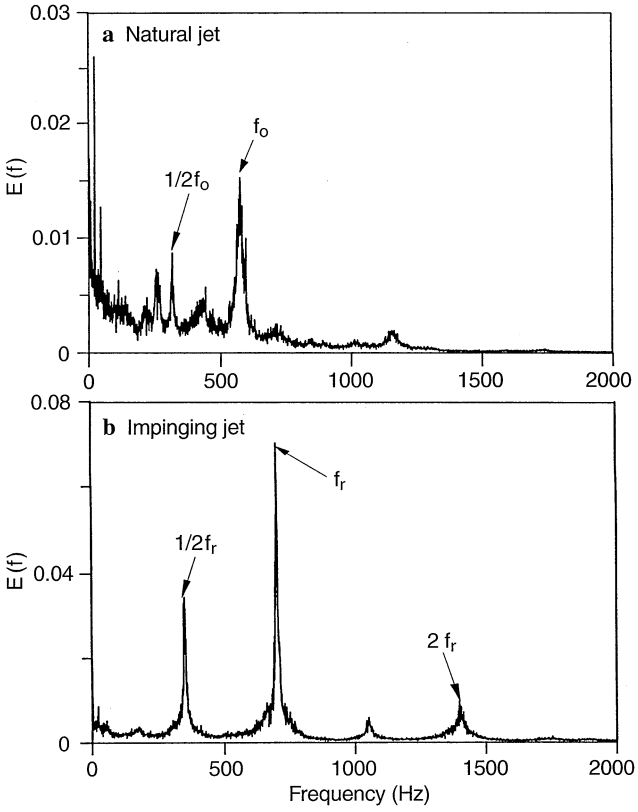

Fig. 5a,b. Energy spectra of instability waves for **a** natural jet, **b** impinging jet at $U_0 = 10$ m/s, $X_{cy} = 0.5$ H and $X = 2\lambda_0$

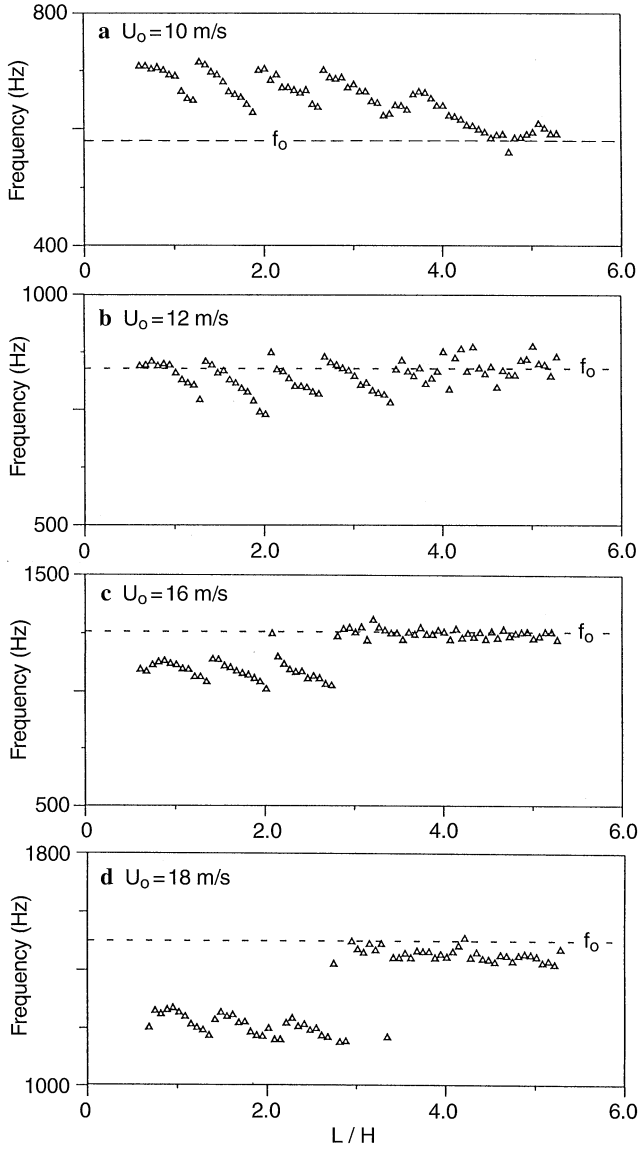

Fig. 6a–d. Variations of resonant frequency according to the impinging length with different jet exit velocities at $X = 2\lambda_0$, $Y = H/2$

core region, the disturbances generated by the cylinder wake can no longer produce effective influence on the evolution of the self-sustained oscillating flow. Under this condition, the resonant frequency is found to be the same as the fundamental frequency of the natural jet, $f_r \approx f_0$. However, higher energy content of the evolving fundamental instability can be obtained (as compared to that of the natural jet) due to enhanced feedback effect from the impinged cylinder. From the measured results shown in Fig. 6, it clearly reveals that the development of the self-sustained oscillating flow and the subsequent evolving coherent structures are significantly affected by the relative positions of the cylinder in the jet column (i.e. within or outside the jet potential core region).

3.2
The characteristics of self-sustained oscillating flow

Recalling the results of Fig. 6, the variations of the resonant frequency are obtained as the small cylinder moves along the streamwise direction of the jet centerline (the detecting single-wire probe is fixed at $2\lambda_0$ from the jet exit). It is noted that the induced flow structures between the jet exit and the cylinder can be divided into several discontinuous stages due to the frequency jump behaviors. According to the feedback mechanism proposed by Ho and Nosseir (1981) for the jet impinges on a flat plate, the governing feedback equation can be written as

$$\alpha = \frac{L}{\lambda_r} + \frac{L}{\lambda_i} \tag{1}$$

where $\lambda_r = U_c/f_r$ and $\lambda_i = a^*f_r$. While α, L, and a denoting wave number, impinging distance and speed of sound, respectively, then Eq. (1) becomes

$$\alpha = f_r\left(\frac{L}{U_c} + \frac{L}{a}\right) \tag{2}$$

As $a \gg U_c$ in subsonic flow,

$$\alpha \cong \frac{f_r L}{U_c} = \frac{f_r L}{KU_0} \tag{3}$$

Here $U_c = KU_0$. The wave number, α, must be an integer under the resonant condition and remains constant until the frequency jump occurs. When the wave number keeps constant, the resonant frequency decreases as the impinging length is increased. Discrete variation of the resonant wave numbers then leads to the resonant frequency jumping accordingly. Moreover, the position of the frequency jump,

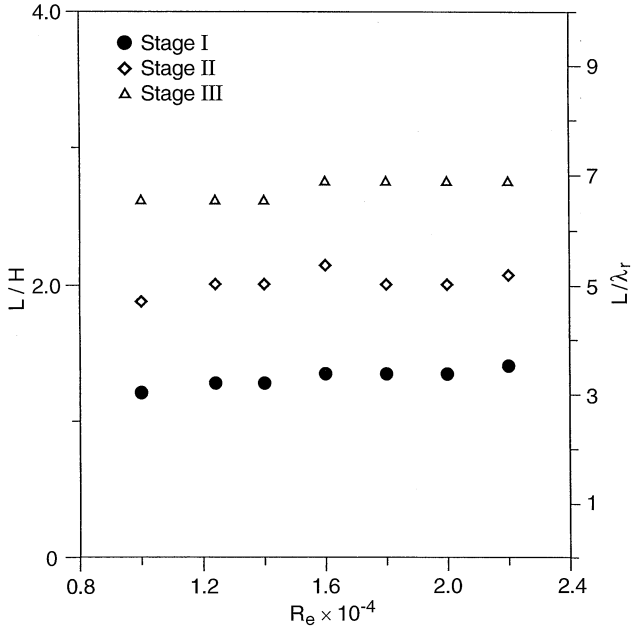

Fig. 7. Cylinder position corresponding to the frequency jump for each stage at various Reynolds numbers

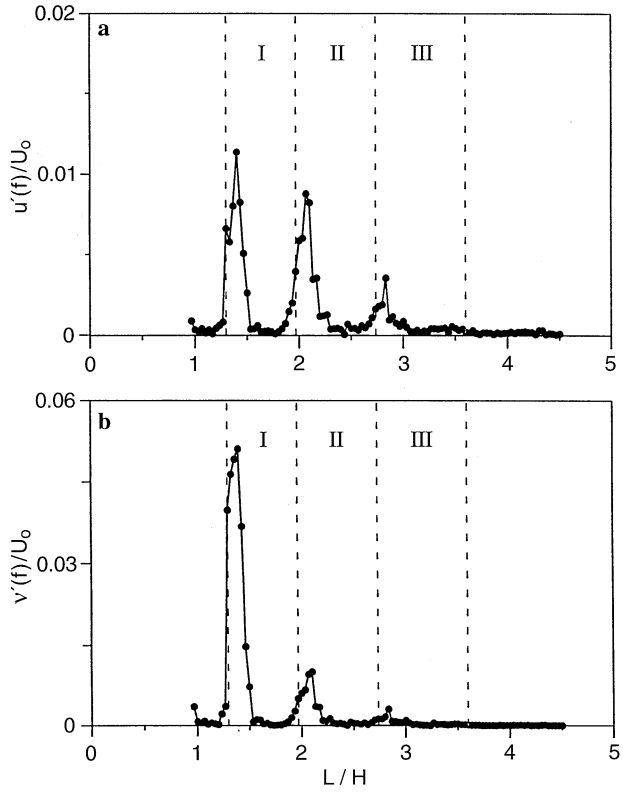

Fig. 9a,b. Evolution of the amplitudes of resonant frequency instabilities for **a** $u'(f_r)$, **b** $v'(f_r)$ at various impinging lengths at $X = 2\lambda_0$, $Y = H/2$

L/*H*, is found to be independent of the Reynolds number. Figure 7 also depicts that the resonant frequency jump positions for each stage related to the impinging length are independent of the jet exit velocity. This is in good agreement with the theorem based on the feedback mechanism.

In the present jet impinging flow field, the upstream propagating disturbances are in the form of pressure wave from the cylinder surface generated by the shedding vortices. The initial most amplified instability is thus excited under the shedding vortex induced disturbances, and then governs the downstream evolution of the coherent structures associated with the self-sustained flow oscillation. The induction mechanism of the self-sustained oscillating flow can then be pictorially illustrated in Fig. 8. The disturbances produced by the cylinder wake would propagate upstream to excite the thin shear layers near the jet exit, and then lead to the formation and evolution of the coherent structures. The control parameters are found to be the resonant frequency (f_r) and the jet convection speed (U_c).

By using a cross-wire sensor, the growth of the streamwise and transverse velocity fluctuations of resonant instabilities is detected at different impinging lengths. Figure 9 shows that the local saturation for the energy of resonant instabilities matches with the initial position of each frequency jump stage, in which the resonant frequency reaches local maximum and is equal to the cylinder wake shedding frequency. Here, by placing the

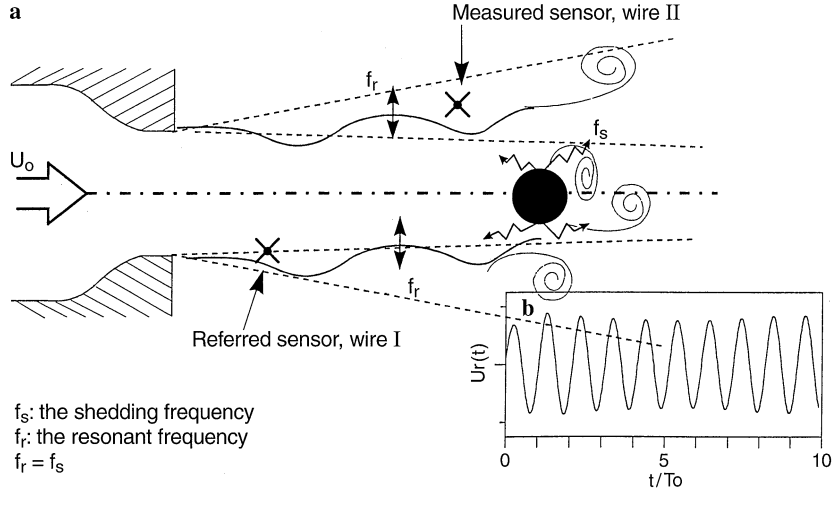

Fig. 8a,b. Schematic diagram of **a** the instrument, **b** the detected reference velocity signal

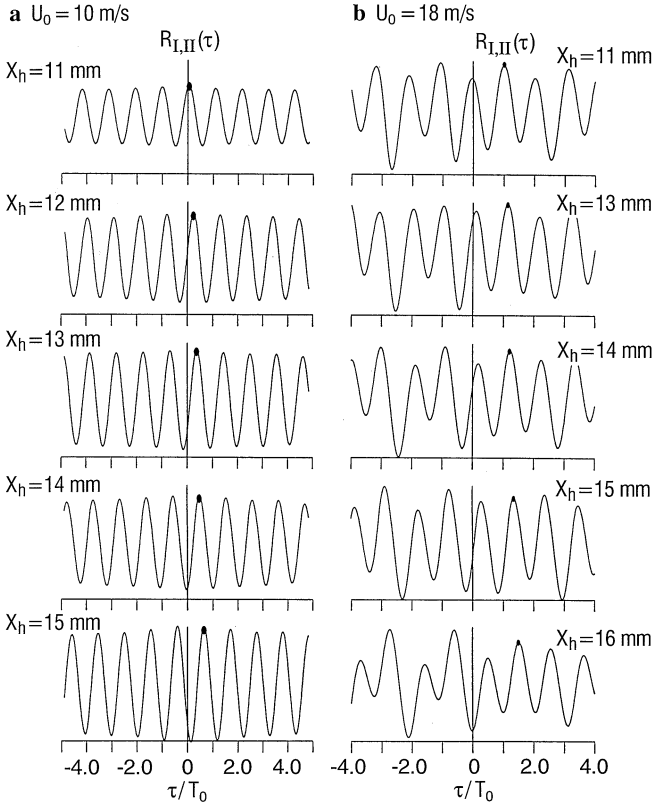

Fig. 10a,b. The cross-correlation coefficient of the velocity signals at different streamwise positions, **a** $U_0 = 10$ m/s, **b** $U_0 = 18$ m/s.

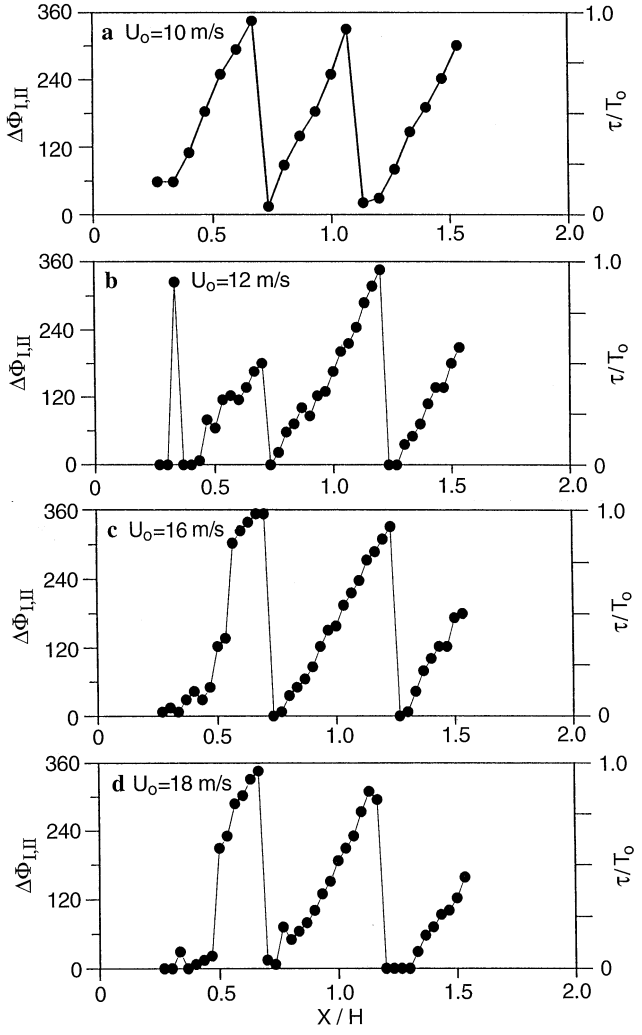

Fig. 11a–d. Variations of time delay at various streamwise positions **a** $U_0 = 10$ m/s **b** $U_0 = 12$ m/sc **c** $U_0 = 16$ m/s **d** $U_0 = 18$ m/s.

cylinder at $X = 1.3H$ of the jet centerline, the amplitude growth of the peak frequency (i.e. the resonant frequency) attains its maximum value such that a self-sustained oscillating flow can be obtained. Based on the feedback mechanism, the dominated instability frequency of the coherent structures is consistent with the frequency of the exciting source in the interaction region. In doing so, the flow can keep a self-sustained situation when the resonant frequency keeps the same as the shedding frequency of the cylinder wake.

In the present study, a single-wire sensor is also used as a reference signal located at the lower shear layer region (labeled as wire *I* shown in Fig. 8). Now, the cross-wire (wire II) is moving along the upper shear layer to measure the characteristics of the flow field. The cross-correlation coefficient, $R_{\mathrm{I,II}}(\tau)$, between the two hot wires I and II, in the resonant impinging flow field is found to perform a sinusoidal oscillation pattern, as shown in Fig. 10. Note that the offset of the local sinusoidal peak represents the relative time (or phase) delay of the two detecting signals. When the hot wire II moves farther away from the reference wire I, the delay time may increase accordingly. Their phase difference $\Delta\phi_{\mathrm{I,II}}$ is expressed in terms of

$$\frac{\Delta\phi_{\mathrm{I,II}}}{2\pi} = \frac{\tau}{T_0} \tag{4}$$

The delay time and phase difference variations at different streamwise positions are plotted in Fig. 11. Note that a periodic (coherent) behavior of the phase difference variation is clearly observed, and the slope of the phase difference change with respect to the measuring position remains constant. It reveals that the induced resonant instabilities here exhibit in the form of a succession of organized vortical structures, which govern the subsequent self-sustained flow oscillations.

The following describes various procedures for determining the wavelengths of the resonant instabilities with the aid of Fig. 11(a):

(I) There are three events to calculate the phase differences from the local minima to the local maxima within the region from the jet exit to the cylinder (i.e. the impinging length). Then the wavelength can be calculated by

$$\lambda_r = \frac{L}{3} = \frac{1.2 \times 15}{3} = 6.0 \text{ mm}.$$

(II) The spatial extensions in each stage of phase difference changes are nearly the same, so $\lambda_r = 6.0$ mm.

(III) From the Rayleigh theorem for a parallel two-dimensional inviscid flow (Rayleigh 1880), the basic steady flow is of the form $U = U(y)$ in the streamwise direction, and the instantaneous velocity fluctuation can be written as

$$u'(x,y,t) = \hat{u}(y)\mathrm{e}^{\mathrm{i}(\alpha x - ct)} \tag{5}$$

where $\hat{u}(y)$ is the amplitude distribution in the transverse direction, $\alpha = \alpha_r + i\alpha_i$ the complex wave number, and c the growth rate. With the assumptions above, it is now possible to estimate the propagating wave characteristics from the measured data. From Eq. (5), the velocity ratio at the two streamwise locations acquired from the hot wire I and II can be derived as

$$\frac{u'(x_2,y,t)}{u'(x_1,y,t)} = \exp\{-[\alpha_i(x_2 - x_1) + i\alpha_r(x_2 - x_1)]\} \quad (6)$$

Let ϕ_u be the phase of u, Eq. (6) can be rewritten as

$$\phi_u(x_2, y, t) = \phi_u(x_1, y, t) + \alpha_r(x_2 - x_1) \quad (7)$$

Therefore,

$$\lambda_r = \frac{2\pi}{\alpha_r} = \frac{2\pi(x_2 - x_1)}{\phi_u(x_2) - \phi_u(x_1)} \approx 6.0 \text{ mm} \quad (8)$$

To sum up, the wavelength of the vortex structures in the self-sustained oscillating flow field should be equal to 6.0 mm. Since the corresponding resonant frequency is 700 Hz as measured in Fig. 4b, the phase velocity becomes $U_c = f_r \times \lambda_r = 700 \times 6.0 = 4.2$ m/s.

In the case of impinging length $L = 1.2H$ here, the wave number is $\alpha = L/\lambda_r = 1.2 \times 15/6.0 = 3$. It performs an integer, which is consistent with the theorem proposed by Ho and Nosseir (1981). Based on the criterion that the values of wavelength at the beginning of each stage are the same, the Eq. (3) can be rewritten in the form

$$\frac{\alpha_{i+1}}{\alpha_i} = \frac{L_{i+1}}{L_i} \quad (9)$$

where subscript i denotes the stage number. Therefore, the wave numbers are 3, 5, and 9 in each stage, respectively. Recalling Eq. (3) derived from the feedback mechanism associated with Fig. 7, the position of the frequency jump is independent of the jet exit velocity. In other word, the maximum impinging length of each stage where the frequency jump occurs would not change for different jet exit velocities.

Recalling Eq. (3) again, the wave number remains constant due to linear relationship between U_0 and f_r. Accordingly, the wave number and the wavelength of the self-sustained oscillating flow are both independent of the jet exit velocity. As a result, the eigenvalue of λ_r is also independent of the Reynolds number of the jet flow. Figures 11(a)–(d) present the variations of phase difference (time delay) at different measuring position for jet exit velocities from $U_0 = 10$–18 m/s. Their distributions are all in similar pattern.

In summary, for the jet-cylinder impinging flow field, the eigenvalues of wavelength, wave number, and phase velocity for the induced self-sustained oscillating flow are shown in Table 1 and Fig. 12. All of these eigenvalues are proven to be independent of the jet exit velocity. Thus, the results of the self-sustained oscillating flow under a specific test condition can also be extended to identify the flow characteristics at other velocities.

Table 1. Summarized instability properties of the self-sustained oscillating flow

Velocity (m/s)	f_0 (HZ)	f_s (Hz)	f_r (Hz)	λ_r (mm)	$U_c = f_r \cdot \lambda_r$ (m/s)	$K = U_c/U_0$
$U_0 = 10$	540	700	700	6.0	4.2	0.42
$U_0 = 12$	700	840	840	6.0	5.04	0.42
$U_0 = 16$	1216	1120	1050	6.0	6.3	0.40
$U_0 = 18$	1450	1260	1200	6.0	7.2	0.40

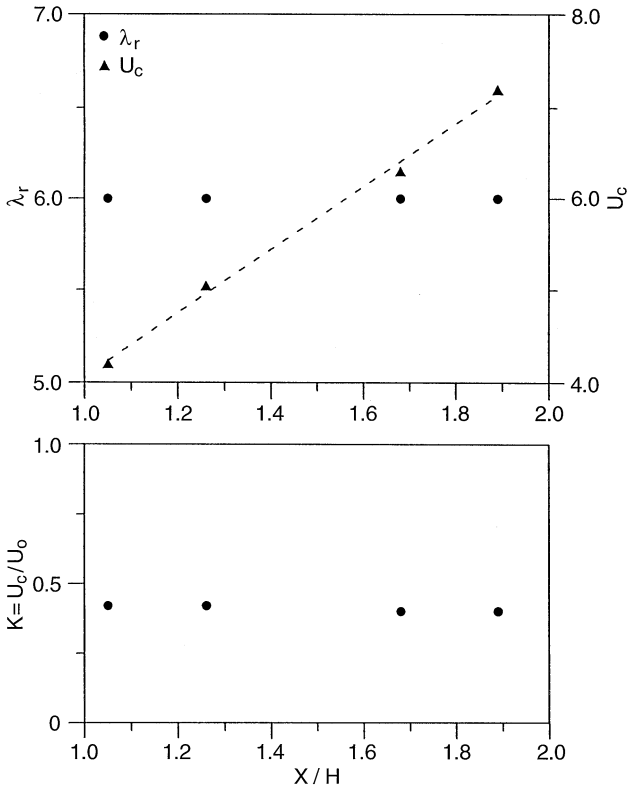

Fig. 12. Flow properties of the self-sustained oscillating flow

4 Concluding remarks

The plane jet impinging upon a small cylinder located in the jet potential core region is extensively studied by hot wire measurements. The resonant frequency of the induced self-sustained oscillating flow is found to match with the vortex shedding frequency produced from the cylinder wake. It is different from the shear layer fundamental instability dominated self-sustained oscillating flow patterns, which occur in the larger obstacle and shear layer impingement case. In other words, the impinged cylinder could be considered to be "small" when its diameter is relatively smaller as compared with the local width of the jet potential core where the cylinder is placed. The instabilities of the cylinder wake now dominate the characteristics of the self-sustained oscillations over the entire flow field. This is primarily due to the jet potential core provides a uniform flow passing through the submerged small cylinder, and this would generate more energized shedding vortices than that from the shear flow field passing upon

the relatively larger impinging obstacles. It reveals that the pressure fluctuation on the cylinder surface performs the upstream-propagating disturbance in the feedback loop of the shear flow field, such that its resonant frequency is well locked to the cylinder wake shedding frequency.

Moreover, the frequency jump behaviors of the self-sustained oscillations are observed to occur at the same position even for different jet exit velocities. In addition, their corresponding wavelengths and wave numbers also remain invariant under the four jet exit velocities tested. These results are in good agreement with the the feedback mechanism by Ho and Nosseir (1981), which stated that the resonant frequency, the wave number in each stage, and the wavelength were all indepentent of the jet exit velocities. From the other viewpoint, it is well known that the Strouhal number of the cylinder wake flow may keep constant as the Reynolds number is large enough. This means that the resulting wavelength should almost be Reynolds number independent. The present calculated Strouhal numbers (St_r) based on the resonant frequency indeed show nearly a constant value of $St_r = 0.2$ even at different Reynolds number. It is then reasonable that the wavelength would not vary accordingly. As a result, the frequency jump positions and the wave number remain the same regardless of the Reynolds number variations.

References

Brackenridge JB (1960) Transverse oscillating of a liquid jet. J Acoust Soc Am 32: 1237–1242

Chanaud RD; Powell A (1965) Some experiments concerning the hole and ring tone. J Acoust Soc Am 37: 902–911

Chou YW; Cheng CK; Sheu SS; Hsiao FB (1996) Self-sustained oscillating vortices of a planar jet impinging upon a small cylinder. Proceedings of 6th International Symposium on Flow Modeling and Turbulence Measurements, Tallahassee, Florida, USA. Sep. 8–10, 133–140

Ho CM; Nosseir NS (1980) Large coherent structures in an impinging turbulent jet. Turbulent Shear Flows, Berlin: Springer, 2, 297

Ho CM; Nosseir NS (1981) Dynamics of an impinging jet, Part 1: The feedback phenomenon. J Fluid Mech 105: 119–142

Lucas M; Rockwell D (1984) Self-excited jet: upstream modulation and multiple frequencies. J Fluid Mech 147: 333–352

Powell A (1961) On the edge tone. J Acoust Soc Am 33: 395–409

Rayleigh L (1880) On the stability, or instability, of certain fluid motions. Proc London Math Soc 11: 57–70

Rockwell D; Kayayoglu R (1986) Unstable jet-edge interaction Part 1: Instantaneous pressure fields at single frequency. J Fluid Mech 169: 125–149

Rockwell D; Naudascher E (1979) Self-sustained oscillations of impinging free shear layers. Ann Rev Fluid Mech 11: 67–94

Rockwell D; Ziada S (1982) Vortex-leading edge interaction. J Fluid Mech 118: 79–107

Roshko A (1954) On the development of turbulent wakes from vortex streets. NACA Report 1911